

Supporting Information

Concentration-Dependent Ion Correlations Impact the Electrochemical Behavior of Calcium Battery Electrolytes

Nathan T. Hahn,^{a,b,*} Julian Self,^{a,c,d} Darren M. Driscoll,^{a,e} Naveen Dandu,^{a,f} Kee Sung Han,^{a,g}
Vijayakumar Murugesan,^{a,g} Karl T. Mueller,^{a,g} Larry A. Curtiss,^{a,f} Mahalingam
Balasubramanian,^{a,e} Kristin A. Persson,^{a,d,h} Kevin R. Zavadil^{a,b}

^aJoint Center for Energy Storage Research, Lemont, IL, 60439

^bMaterial, Physical and Chemical Sciences Center, Sandia National Laboratories, Albuquerque, NM 87185

^cEnergy Technologies Division, Lawrence Berkeley National Laboratory, Berkeley, CA 60439

^dDepartment of Materials Science and Engineering, UC Berkeley, CA 94720

^eAdvanced Photon Source, Argonne National Laboratory, Lemont, IL, 60439

^fMaterials Science Division, Argonne National Laboratory, Lemont, IL, 60439

^gPhysical and Computational Sciences Directorate, Pacific Northwest National Laboratory, Richland, WA 99354

^hMolecular Foundry, Lawrence Berkeley National Laboratory, Berkeley, CA 94720

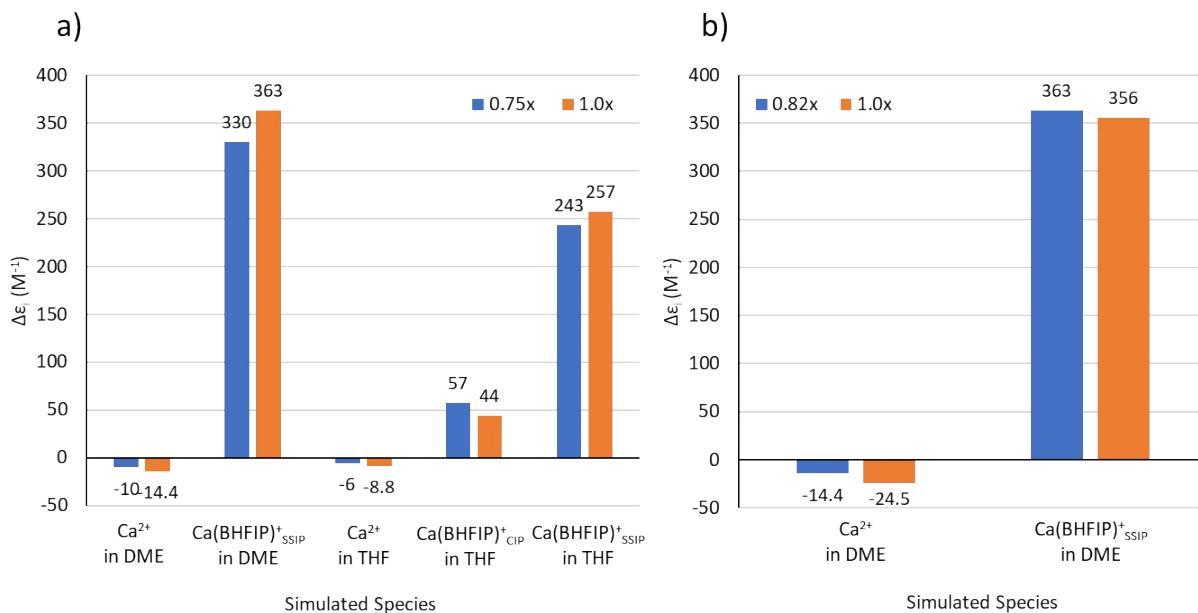


Figure S1. Calculated species dielectric increments derived from species-constrained MD as a function of a) ionic charge scaling (e.g. calcium ionic charge 1.5 versus 2.0, etc.) and b) solvent charge scaling (i.e. partial charges on atoms of solvent molecule). The dielectric increment sign and general magnitude are preserved.

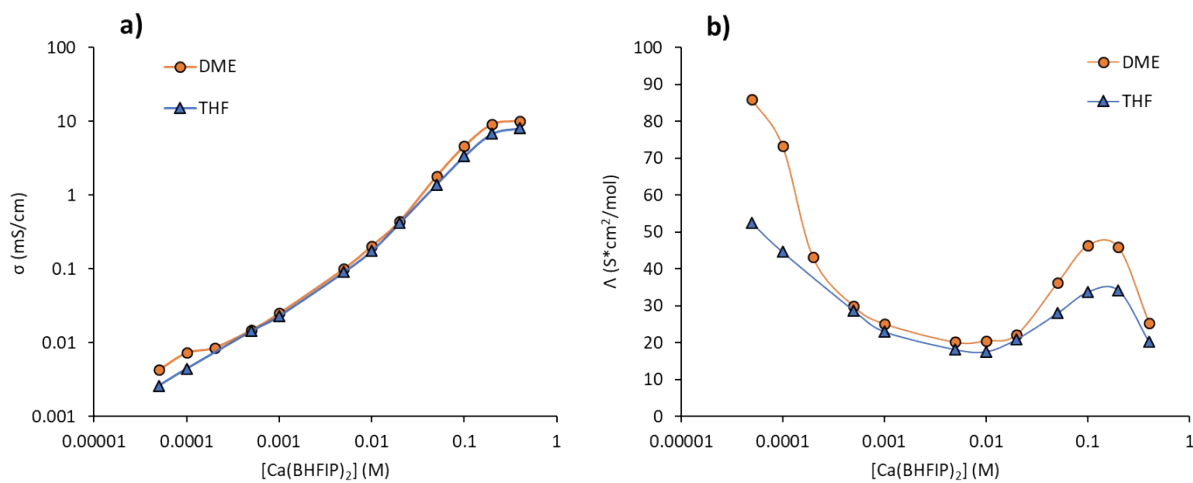


Figure S2. a) Conductivity and b) molar conductivity measurements across five decades of $Ca(BHFIP)_2$ concentration in DME and THF.

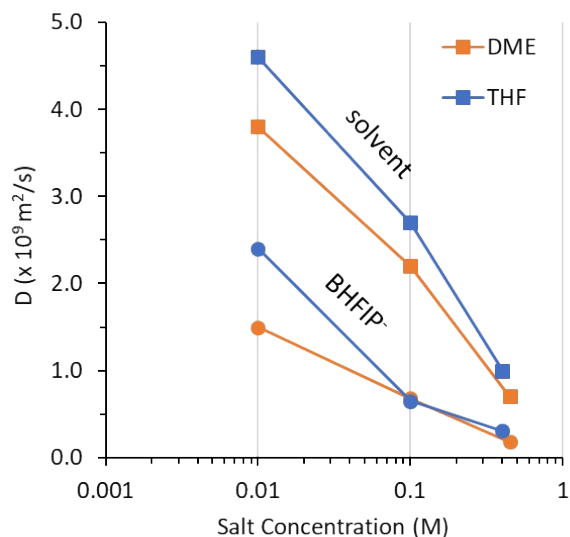


Figure S3. Self-diffusion coefficients measured by PFG-NMR for the solvents (■) and anions (●) in solution as a function of $\text{Ca}(\text{BHFIP})_2$ concentration in DME and THF.

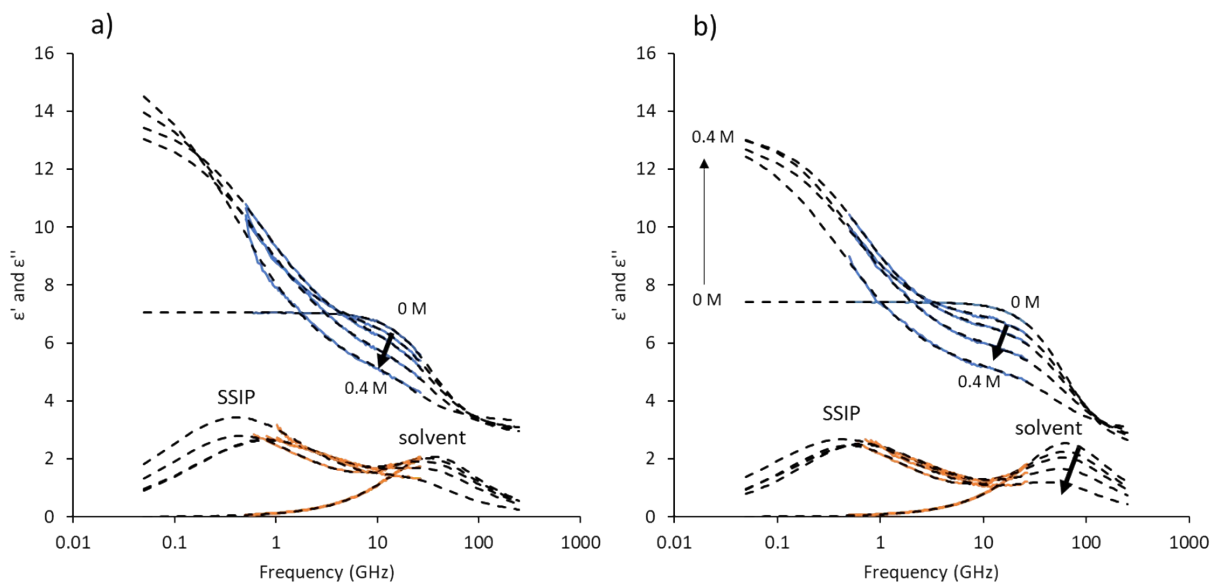


Figure S4. Complex permittivity spectra measured by DRS at 0, 0.05, 0.1, 0.2, and 0.4 M $\text{Ca}(\text{BHFIP})_2$ concentrations in a) DME and b) THF. Blue curves represent ϵ' and orange curves represent ϵ'' while the dashed lines represent simultaneously derived, extrapolated fits containing one Debye and one Cole-Cole relaxation. At elevated concentrations the free solvent dipole amplitude (ϵ_{solv}) decreases substantially due to irrotational binding to Ca^{2+} as well as a reduced solvent mole fraction in solution. This causes the overall ϵ_r to level-off despite a general increase in the SSIP amplitudes.

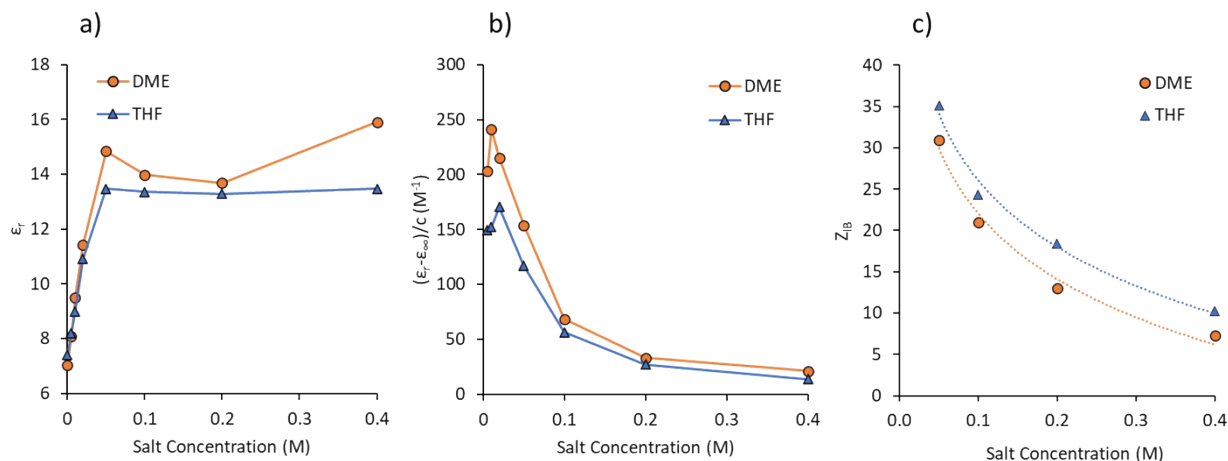


Figure S5. a) Solution dielectric constants extracted from the DRS spectra. b) Effective solution dielectric increments calculated by dividing the DRS-measured dipole dispersion amplitude by the salt concentration. Values above 45 can only be explained by the formation of significant SSIP populations. c) Average numbers of irrotationally bound solvent molecules per salt unit (Z_{IB}) derived from changes in ϵ_{solv} , including the effects of kinetic depolarization and following the methodology described by Buchner et al.¹⁻² Logarithmic trend lines are included to guide the eye. The lowest concentrations are excluded from this analysis as small changes in ϵ_{solv} lead to large uncertainties in Z_{IB} . These calculations demonstrate that each Ca^{2+} interacts with solvent molecules beyond its first solvation shell, especially at lower concentrations. At high concentrations these values begin to approach the expected Ca^{2+} -solvent first shell solvent coordination numbers of 4 (DME) and 6 (THF).

Table S1. DRS parameters extracted from spectral fitting of $\text{Ca}(\text{BHFIP})_2 / \text{DME}$ solutions using one Debye and one Cole-Cole relaxation.

Concentration (M)	$\sigma_{\text{eff}}^{\text{a}}$ (mS/cm)	ϵ_r	ϵ_{∞}	ϵ_{DME}	τ_{DME} (ps) ^b	ϵ_{SSIP}	τ_{SSIP} (ps)	$\alpha_{\text{SSIP}}^{\text{c}}$
0.00		7.0	2.9	4.2	4.5			
0.005	0.11	8.1	2.9	4.1	4.5	1.1	272	0.10
0.01	0.22	9.5	2.9	4.0	4.5	2.6	296	0.16
0.02	0.40	11.4	2.9	3.8	4.5	4.6	358	0.21
0.05	1.50	14.8	3.0	3.4	4.5	8.4	371	0.27
0.10	4.17	14.0	3.0	2.9	4.5	8.1	214	0.27
0.20	8.87	13.7	2.9	2.3	4.5	8.5	204	0.30
0.40	10.11	15.9	3.3	1.5	7.0	11.1	398	0.30

^aDerived from DRS fitting

^b $\tau = 1/(2\pi f)$, constrained as \geq the neat solvent value

^cConstrained ≤ 0.30

Table S2. DRS parameters extracted from spectral fitting of $\text{Ca}(\text{BHFIP})_2 / \text{THF}$ solutions using one Debye and one Cole-Cole relaxation.

Concentration (M)	$\sigma_{\text{eff}}^{\text{a}}$ (mS/cm)	ϵ_{r}	ϵ_{∞}	ϵ_{THF}	τ_{THF} (ps) ^b	ϵ_{SSIP}	τ_{SSIP} (ps)	$\alpha_{\text{SSIP}}^{\text{c}}$
0.00		7.4	2.3	5.1	2.5			
0.005	0.09	8.2	2.4	5.0	2.5	0.9	285	0.05
0.01	0.17	9.0	2.4	4.9	2.5	1.7	305	0.09
0.02	0.38	10.9	2.4	4.8	2.5	3.7	342	0.15
0.05	1.29	13.5	2.6	4.2	2.5	6.7	336	0.20
0.10	3.09	13.4	2.7	3.7	2.5	7.0	242	0.21
0.20	6.34	13.3	2.8	2.8	2.5	7.7	247	0.28
0.40	8.00	13.5	3.0	1.8	3.2	8.7	374	0.30

^aDerived from DRS fitting

^b $\tau = 1/(2\pi f)$, constrained as \geq the neat solvent value

^cConstrained ≤ 0.30

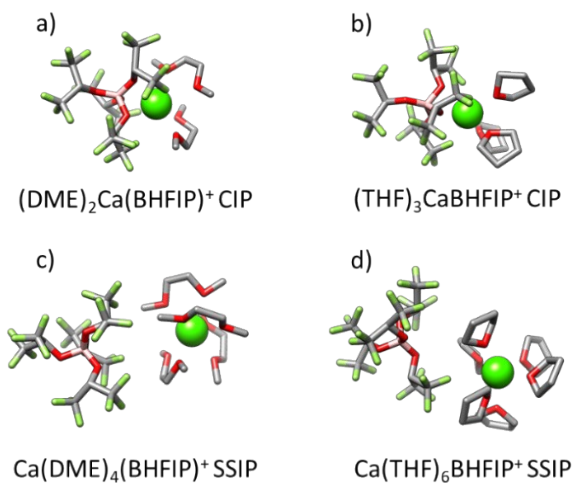


Figure S6. Representative ion pair structures from MD simulations corresponding to both a,b) contact-ion pairs (CIPs) and c,d) solvent-separated ion pairs (SSIPs) in a,c) DME and b,d) THF. Atoms of Ca, B, O, C, and F are depicted as bright green, pink, red, grey, and light green, respectively. H atoms and 2nd shell solvent are omitted.

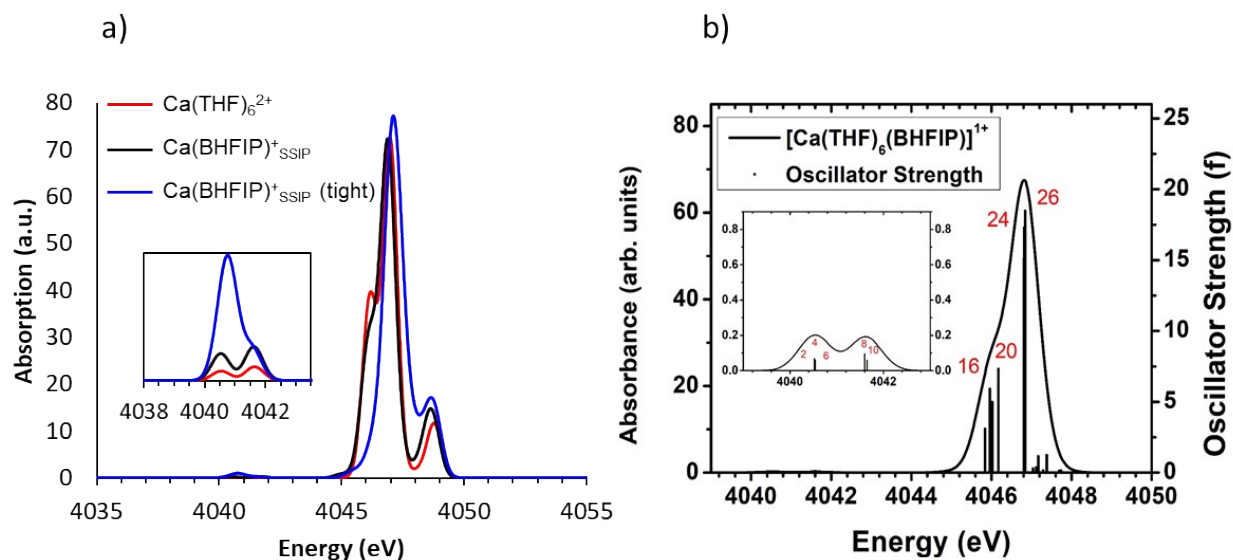


Figure S7. a) Computed X-ray absorbance spectra illustrating the impact of “tight” Ca^{2+} -BHFIP⁻ binding in the SSIP cluster. b) Computed X-ray absorbance spectrum of the “loose” SSIP cluster in the presence of THF as an implicit solvent constructed using CPCM model. Individual excited state contributions to the absorbance are numbered and correspond to the assignments shown in Tables S3 and S4. Pre-edge states are magnified for clearer visualization.

Table S3. Pre-edge peak Natural Transition Orbitals (NTOs) and their contributions in presence of THF CPCM model. Excited state energies are corrected by +50.4 eV to align with the experimental energies.

Excited State	Excited State energy (eV)	NTO Hole	NTO Contributions (threshold = 0.3)
2	4040.525		Ca 1s → Ca 3d (24.9 %) (Mostly Ca 3d _{xy})
4	4040.527		Ca 1s → Ca 3d (24.0 %) Ca 4p (2.2 %) (Mostly Ca 3d _{yz})

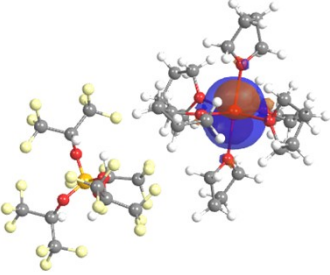
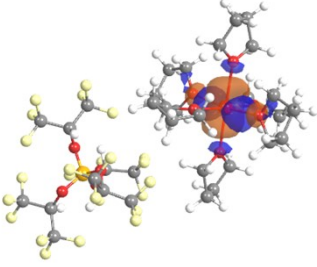
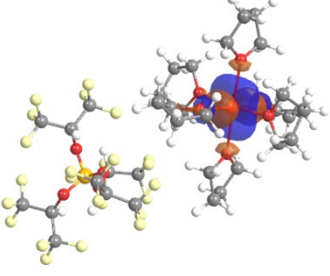
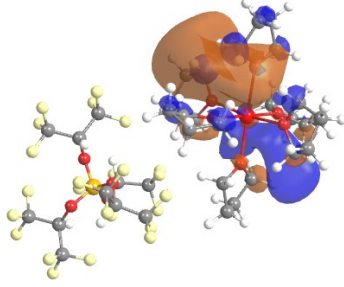
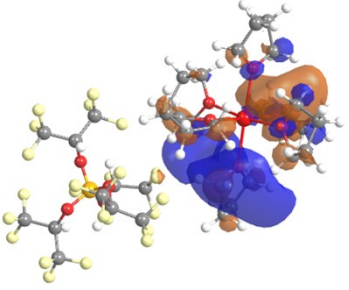
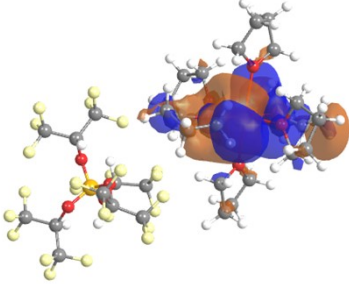
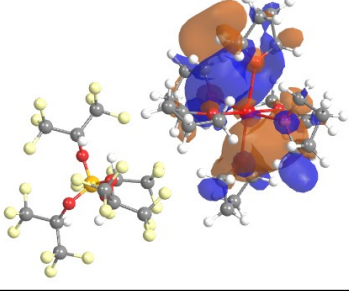
6	4040.543		Ca 1s → Ca 3d (28.1 %) (Mostly Ca 3d _{z²})
8	4041.598		Ca 1s → Ca 3d (12.9 %) C 3p (7.1 %) (Mostly Ca 3d _{x²-y²})
10	4041.552		Ca 1s → Ca 3d (17.3 %) C 3p (1.5 %) (Mostly Ca 3d _{xz})

Table S4. Rising edge peak NTOs and their contributions in presence of THF CPCM model. Excited state energies are corrected by +50.4 eV to align with the experimental energies.

Excited State	Excited State energy (eV)	NTO Hole	NTO Contributions (threshold > 1 %)
16	4045.956		Ca 1s → Ca - 4p (38.5%) C - 3s (1.9 %) C - 3p (3.6 %) H - 2s (3.7 %)

20	4046.166		<p>Ca 1s → Ca – 4p (26.3 %) Ca – 4s (2.2 %) C – 3p (2.9 %) H – 2s (3.6 %)</p>
24	4046.821		<p>Ca 1s → Ca – 3d (3.5 %) Ca – 4p (4.3 %) C – 3p (2.1 %) H – 2s (3.4 %)</p>
26	4046.843		<p>Ca 1s → Ca – 3d (14.7 %) Ca – 4p (5.3 %) O – 3s (1.2 %) C – 3p (8.6 %)</p>

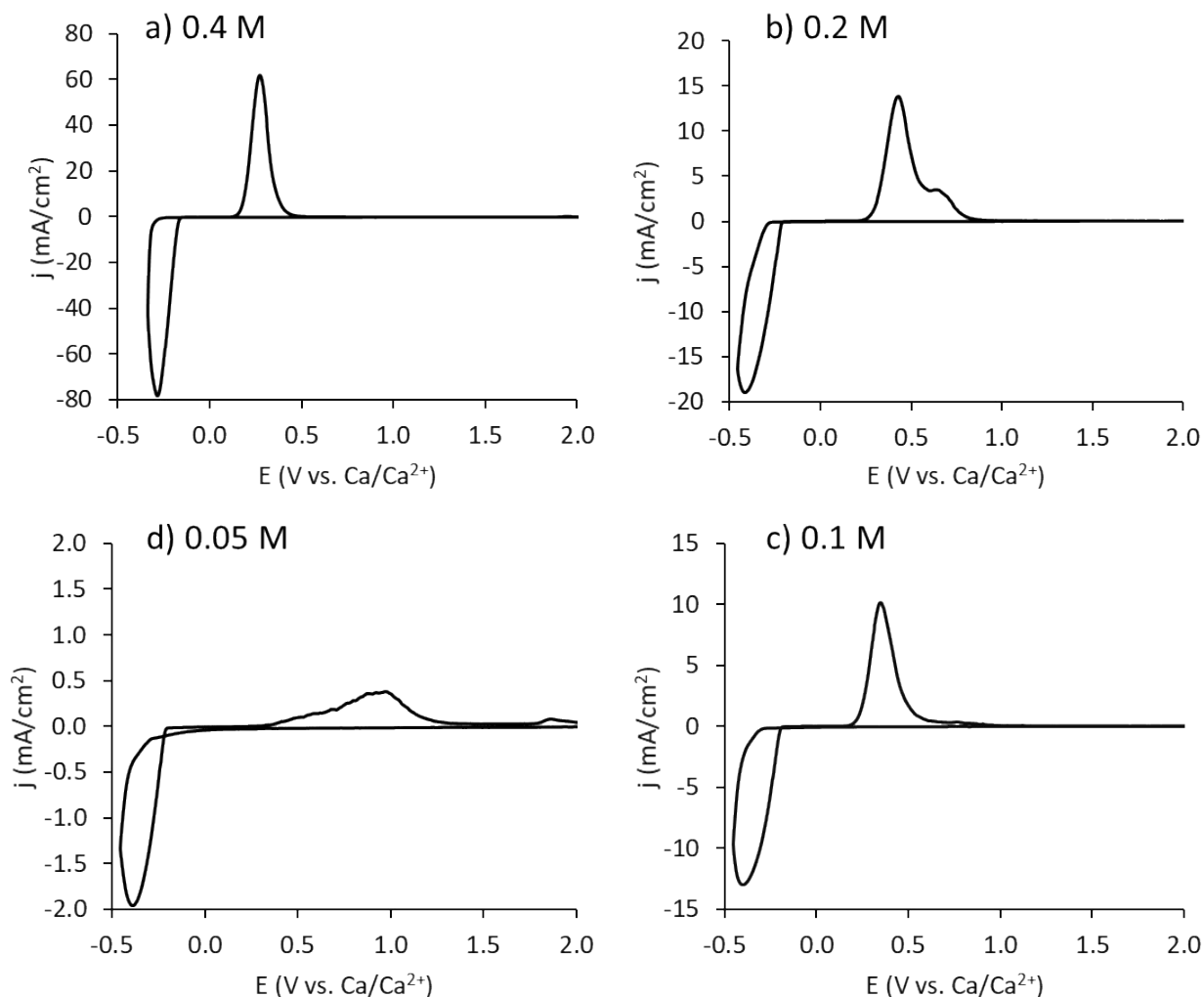


Figure S8. Representative cyclic voltammograms of calcium cycling on gold measured at various concentrations of Ca(BHFIP)₂ in DME. The potential scan rate is 50 mV/s and IR correction was applied in each case. These curves were generated within the first 3-5 cycles to avoid excessive electrode modification. Aside from the 0.4 M data, all the CVs exhibit a somewhat distributed stripping peak, indicative of non-uniform surface passivation.

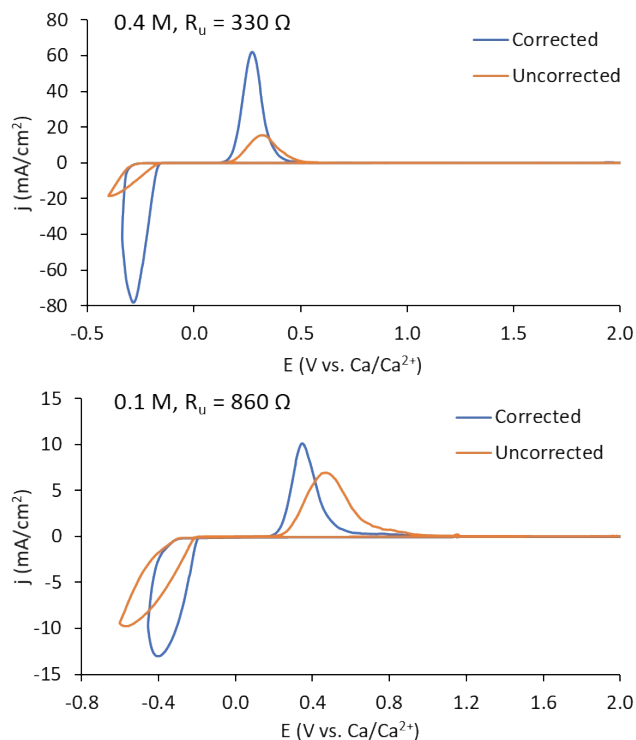


Figure S9. Representative cyclic voltammograms of calcium cycling on gold in a 3-electrode cell measured at 0.4 and 0.1 M $\text{Ca}(\text{BHFIP})_2$ in DME demonstrating the effects of IR correction. Uncompensated resistance (R_u) was measured via electrochemical impedance spectroscopy prior to the CV measurements and was used by the potentiostat software to actively correct the reference potential during the CV. The potential scan rate is 50 mV/s.

1. Buchner, R.; Hefter, G. T.; May, P. M., Dielectric Relaxation of Aqueous NaCl Solutions. *The Journal of Physical Chemistry A* **1999**, *103* (1), 1-9.
2. Buchner, R.; Chen, T.; Hefter, G., Complexity in “simple” electrolyte solutions: Ion pairing in $\text{MgSO}_4(\text{aq})$. *The Journal of Physical Chemistry B* **2004**, *108* (7), 2365-2375.